Rare Metal Materials and Engineering
Volume 50, Issue 5, May 2021
Available online at www.rmme.ac.cn

Science Press

Cite this article as: Hong Dan, Jiao Zhen, Zeng Wei, et al. Electronic Structure and Relative Stability of Nb_2Al (100) Surfaces[J]. Rare Metal Materials and Engineering, 2021, 50(05): 1596-1601.

ARTICLE

Electronic Structure and Relative Stability of Nb_2Al (100) Surfaces

Hong Dan[1,3], Jiao Zhen[1,3], Zeng Wei[2], Liu Fusheng[1,3], Tang Bin[4], Liu Qijun[1,3]

[1] Key Laboratory of Advanced Technologies of Materials, Ministry of Education, School of Physical Science and Technology, Southwest Jiaotong University, Chengdu 610031, China; [2] College of Medical Technology, Chengdu University of TCM, Chengdu 610075, China; [3] Sichuan Provincial Key Laboratory (for Universities) of High Pressure Science and Technology, Southwest Jiaotong University, Chengdu 610031, China; [4] State Key Laboratory of Solidification Processing, Northwestern Polytechnical University, Xi'an 710072, China

Abstract: The electronic structures, surface energies and thermodynamic properties of different terminated Nb_2Al (100) surfaces were studied using first-principle calculations based on density functional theory. Results show that the calculated electronic structures present the enhanced metallic character and decrease covalent character for all terminated surfaces, which are attributed to the surface relaxations and the formation of surface states. According the calculated surface energies of different terminations, the surface stabilities of non-stoichiometric surfaces were analyzed. The C terminated surface ($Nb_{22}Al_{12}$) is the most thermodynamically stable surface under both Nb-rich and Al-rich conditions. Moreover, the work function of Nb_2Al (100) surface was calculated, indicating that its ability to gain and lose electrons on the surface is similar to that of pure elemental surface before formation.

Key words: intermetallic; density functional theory; electronic structure; surface properties

With the advance of society, the high-temperature structural materials attract scientists' attention. The niobium-aluminum intermetallic compounds show low density, high melting point and good high temperature yield strength and are widely investigated[1-4]. The main research objects of niobium-aluminum intermetallic compounds include Nb_3Al, Nb_2Al and $NbAl_3$. Nb_3Al is widely studied due to its high field superconducting properties[5]. The relatively low density, high melting point and good compatibility with Al_2O_3 fibers of $NbAl_3$ also have attracted researchers' wide interests[6]. However, Nb_2Al is barely investigated. The special physical properties of Nb_2Al, such as the brittle-ductile transition temperature (BDTT) and the yield strength[7,8], need further investigation.

Structural properties of Nb_2Al have been studied[9-12]. Monolithic Nb_2Al is very brittle[1,2,8], so the eutectic alloy Nb_2Al-Al_3Nb was fabricated[13,14]. In the eutectic alloy, Rios et al[13] found that Nb_2Al preferably grows along the (210) and (420) directions and Al_3Nb preferably grows along the (004) direction by X-ray diffraction analysis. The eutectic alloy shows high strength at high temperature and low fracture toughness at room temperature[14]. The improvement of the fracture toughness is very important for its high temperature applications[15-18]. Recently, the mechanical properties of Nb_2Al under pressure[19] were studied. However, the information about its surface properties and stabilities, which are closely related with the high-temperature oxidation resistance, is still lacking.

Due to its complicated crystal structure, the surface properties and stabilities of Nb_2Al are difficult to characterize and obtain[20]. First-principle calculations provide a method to investigate surface properties of Nb_2Al and agree well with the experimental studies. The surface performance and stability of Nb_2Al were further studied by the first-principle calculation method based on the density-functional theory in this research. Different atom-terminated models of Nb_2Al (100) surfaces were under consideration. The surface electronic structures, surface energies and thermodynamic stability of Nb_2Al (100) surfaces were investigated by the first-principle calculations.

1 Computational Methods and Models

All simulations in this research were performed by first-

Received date: May 18, 2020
Foundation item: Sichuan Science and Technology Program (2018JY0161); Fundamental Research Funds for the Central Universities (2682019LK07); State Key Laboratory of Solidification Processing in NWPU (SKLSP201843)
Corresponding author: Liu Qijun, Ph. D., Associate Professor, School of Physical Science and Technology, Southwest Jiaotong University, Chengdu 610031, P. R. China, E-mail: qijunliu@home.swjtu.edu.cn

principle calculation method based on the density-functional theory as implemented in the CASTEP code[21]. The ultrasoft pseudopotential[22] and the generalized gradient approximation (GGA) with Perdew-Wang 91 (PW91) function[23] were applied. The Brillouin zone integration was sampled using Monkhorst-Park k 1×1×3 and 1×3×1 meshes[24] for bulk Nb_2Al and Nb_2Al (100) surfaces, respectively. The electrons of Nb $4s^24p^64d^45s^1$ and Al $3s^23p^1$ were treated as valences. The plane wave cutoff energy was set as 400 eV in this research, which was already verified to be sufficient for energy convergence. The geometry optimizations stopped until the total energy, maximum force, maximum stress and maximum displacement were less than 5×10^{-6} eV/atom, 0.1 eV/nm, 0.02 GPa and 5×10^{-7} nm, respectively.

Before calculating the surfaces, the bulk properties of Nb_2Al with the most stable tetragonal structure (space group P42/mnm) were optimized[1,2,12]. The obtained lattice parameters were $a=b$=1.000 86 nm and c=0.518 35 nm, which are in agreement with the experimental[9-11,13] and theoretical[12] values. It is suggested that the methods can be used to study the surface properties of Nb_2Al. Since the experiments found that many planar faults appear on (100) and (010) planes of Nb_2Al in the Nb_2Al-$NbAl_3$ eutectic alloy[20], including the vacuum regions and repeated slabs[25,26], the plane slab approach was used and the periodic boundary conditions were applied to different atom-terminated models for Nb_2Al (100) surfaces to model the surfaces of tetragonal Nb_2Al. Fig. 1 shows the surface models with $Nb_{20}Al_{11}$, $Nb_{21}Al_{12}$, $Nb_{22}Al_{12}$, $Nb_{23}Al_{12}$ and $Nb_{25}Al_{12}$ terminations, namely A termination, B termination, C termination, D termination, and E termination, respectively, where the repeated slabs avoid the interaction by vacuum regions of 1.2 nm.

2 Results and Discussion

2.1 Surface relaxations

Due to the complex geometry of bulk Nb_2Al, the overall relaxation of surface is used to describe the structural changes after the surface forms. For A, B, C, D, and E terminations, the overall relaxations are 0.026 87, 0.006 84, 0.018 12, 0.010 58 and 0.015 55 nm, respectively. Moreover, all surfaces relax inwardly.

2.2 Surface electronic properties

Fig. 2 shows the total density of states (TDOS) and partial

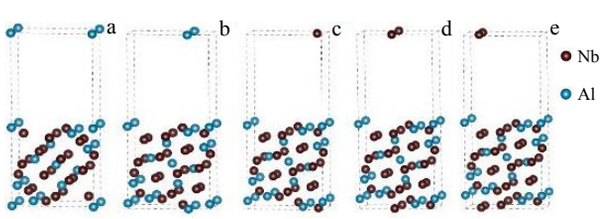

Fig.1 Surface models of Nb_2Al (100) surfaces with A (a), B (b), C (c), D (d), and E (e) terminations

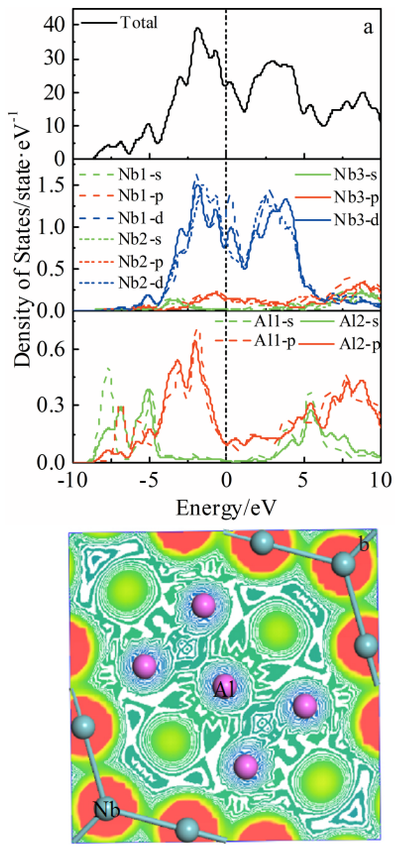

Fig.2 TDOS and PDOS (a) and charge densities (the color from dark green to red represents the transition from a negative charge to a positive charge) (b) of bulk Nb_2Al

density of states (PDOS) of bulk Nb_2Al. In the tetragonal Nb_2Al, it has two and three types of Al and Nb atoms, respectively. The Al1, Al2, Nb1, Nb2 and Nb3 atoms are located at 2*a* (0, 0, 0), 8*i* (0.0665(5), 0.2615(5), 0), 4*f* (0.3965(3), 0.3965(3), 0), 8*i* (0.5350(2), 0.1280(2), 0), and 8*j* (0.1820(2), 0.1820(2), 0.2520(7))[27], respectively. It can be seen that the tetragonal Nb_2Al is a conductive phase due to the TDOS with nonzero value at Fermi level. The metallic conductivity of tetragonal Nb_2Al is mainly due to Nb-4d states. According to the PDOS, it can be seen that the contribution of valence electrons to the bonds around Fermi energy is mainly originated from Nb-4d and Al-3p states. Moreover, a valley named pseudogap[28] appears at the right side of Fermi level, indicating that the covalent bond exists in the tetragonal Nb_2Al due to the Nb-Nb and Nb-Al bonds. For example, the conclusion of Nb-Nb covalent bonds can be further verified by the charge densities, as shown in Fig.2b.

For the surfaces of Nb_2Al, the TDOS and PDOS of different terminations to explore the characteristics of surface states are shown in Fig. 3. All terminations show metallic nature. Comparing with the TDOS of bulk Nb_2Al, the TDOS of all terminated surfaces move to the right side, resulting in the increase of metallic property. The TDOS at Fermi level is 0.742, 1.017,

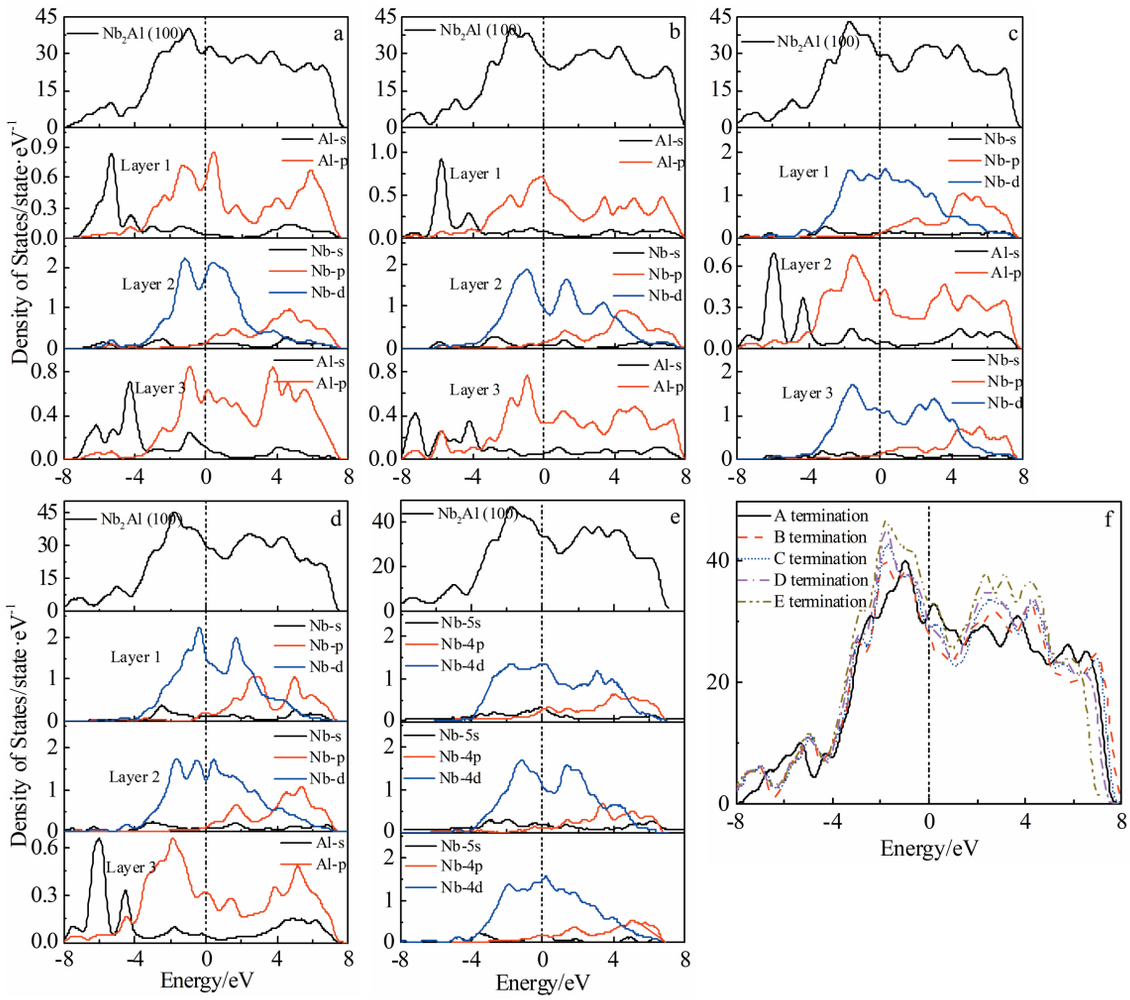

Fig.3 TDOS and PDOS of Nb_2Al (100) surfaces with A (a), B (b), C (c), D (d), and E (e) terminations; comparison of TDOS of different termination surfaces (f)

0.847, 0.854, 0.855, and 0.879 state·eV^{-1} per atom for bulk, A, B, C, D and E terminations, respectively, indicating that the metallic property is enhanced after the surfaces form. Moreover, the contribution to the enhanced metallic property is mainly associated with Al-3p states. Accordingly, the covalent character formed by the hybridization between Nb-4d and Al-3p states decreases. The changed pseudogap in surfaces proves the conclusion. In addition, the covalence of these terminated planes is sorted by B>C>D>E>A according to the width of the pseudogaps in Fig. 3f. To further analyze the chemical bonds of the Nb_2Al (100) surfaces, the bond populations of surfaces and bulk Nb_2Al are calculated. The biggest bond population for the Nb-Nb bonds is 0.66, 0.45, 0.42, 0.56, 0.49, 0.59 e for bulk, A, B, C, D and E terminations, respectively. It is well-known that a high population indicates a high degree of covalence in the bonds[29], i.e., the degree of covalence of Nb-Nb bonds in terminated surfaces decreases. Moreover, after the formation of surfaces, the non-bonding appears between Nb and Nb, further indicating the decreased covalence. The sums of the overlap populations for the outer atoms are 3.45, 5.61, 5.15, 4.64, and 3.63 e for A, B, C, D and E terminations, respectively. It can be seen that this covalence order is consistent with the conclusion of the pseudogaps. The increased metallic property and decreased covalent property are due to the surface relaxations and surface states.

2.3 Surface energies and relative stabilities

The surface energies can be used to estimate the stability of the various surfaces[30-38]. In this work, the symmetric and stoichiometric Nb_2Al (100) surfaces are impossibly built by directly cutting of bulk Nb_2Al. However, the average surface energy of non-stoichiometric surfaces can be obtained by D and E terminated surfaces because the sum of Nb and Al atoms in D and E terminations satisfies the stoichiometric ratio[30]:

$$E_{surf}^{ave} = \frac{1}{4A}\left[E_{slab}^{DTer} + E_{slab}^{ETer} - (N_{Al}^{DTer} + N_{Al}^{ETer})\mu_{Nb_2Al}^{bulk}\right] \quad (1)$$

where the E_{slab}^{DTer} and E_{slab}^{ETer} are the total energies of the fully relaxed D and E terminations, respectively; N_{Al}^{DTer} and N_{Al}^{ETer} are the total number of Al atoms for D and E terminations, respectively; $\mu_{Nb_2Al}^{bulk}$ is the chemical potential of bulk Nb_2Al; A is the area of the 2D cell. The calculated average surface energy of

Nb_2Al (100) is 2.316 J/m^2.

Moreover, the surface energies of stoichiometric surfaces of Nb_2Al can be calculated by Eq.(2)[31-33]:

$$E_{surf}=\frac{1}{2A}(E_{slab}-N_{Nb}\mu_{Nb}^{slab}-N_{Al}\mu_{Al}^{slab}) \quad (2)$$

where E_{surf} is the surface energy; E_{slab} refers to the total energy of the fully relaxed slab; N_{Nb} and N_{Al} are the numbers of Nb and Al atoms in the slab, respectively; μ_{Nb}^{slab} and μ_{Al}^{slab} are the chemical potentials of Nb and Al in the slab, respectively. The chemical potential of bulk state is balanced with one of the surface state[39]: $2\mu_{Nb}^{slab}+\mu_{Al}^{slab}=\mu_{Nb_2Al}^{bulk}$, so the surface energy is defined as follows:

$$E_{surf}=\frac{1}{2A}[E_{slab}-N_{Al}\mu_{Nb_2Al}^{bulk}+(2N_{Al}-N_{Nb})\mu_{Nb}^{slab}] \quad (3)$$

The formation enthalpy (ΔH) of bulk Nb_2Al is obtained by Eq.(4):

$$2\mu_{Nb}+\mu_{Al}+\Delta H=\mu_{Nb_2Al}^{bulk} \quad (4)$$

where μ_{Nb} and μ_{Al} are the chemical potentials of metallic niobium and aluminum, respectively. ΔH=-28.27 kJ/mol per formula unit of bulk Nb_2Al is obtained. The formation enthalpies including the results reported by Papadimitriou[12], Shilo[40] and Gelashvilli[41] at 298 K are listed in Table 1. It can be seen that the calculated value in this research agrees well with Papadimitriou's results, and is slightly bigger than the data of Shilo and smaller than the Gelashvilli's data. Then $\mu_{Al}-\mu_{Al}^{slab}+\Delta H=2\mu_{Nb}^{slab}-2\mu_{Nb}=2(\mu_{Nb}^{slab}-\mu_{Nb})$ is obtained.

Due to the negative formation enthalpy of bulk Nb_2Al and the smaller chemical potential for species, the conditions $\mu_{Al}-\mu_{Al}^{slab}>0$ and $\mu_{Nb}^{slab}-\mu_{Nb}<0$ are shown. Hence, the range of chemical potential for Nb is as follows:

$$\frac{1}{2}\Delta H+\mu_{Nb}<\mu_{Nb}^{slab}<\mu_{Nb} \quad (5)$$

It is worth noting that the surface energies of all non-stoichiometric surfaces depend on the chemical potential of Nb and the stabilities of non-stoichiometric surfaces are correlated with the chemical potential of Nb. Combining Eq.(3) and Eq.(5), the calculated surface energies of different terminations of Nb_2Al (100) are shown in Fig.4. It can be seen that the surface energy of E termination decreases with the increase of $(\mu_{Nb}^{slab}-\mu_{Nb})$, while that of other terminations increases. Under Nb-rich conditions, the surface energy of Nb_2Al (100) with different terminations is in the sequence as follows: A>B>E>D>C. While under Nb-deficient conditions, the order changes to A>E>B>D>C, indicating that the C termination is the most stable surfaces under both Nb-rich and Al-rich conditions. The A termination is the most unstable surface of Nb_2Al (100) surfaces. The stability of A, C, D and E terminations are consistent with the conclusions of 2.2 Section. The decreasing stability of B termination may be related to the activation of the Al atoms in the outermost surface.

Table 1 Formation enthalpy ΔH of bulk Nb_2Al

Formation enthalpy of Nb_2Al, ΔH/kJ·mol^{-1}	Ref.
-28.27 (at 0 K)	Calculated
-28.753 (at 0 K), −28.048 (at 298 K)	[12]
-25.0	[40]
-33.5 (at 298 K)	[41]

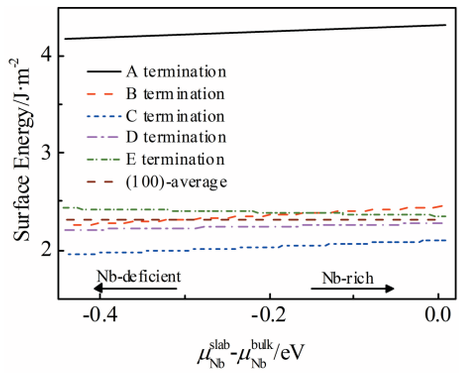

Fig.4 Relationship between surface energy and ($\mu_{Nb}^{slab}-\mu_{Al}^{slab}$)

Table 2 Work function Φ for Al, Nb and Nb_2Al (100)

Sample	Work function/eV	Ref.
Al	3.87	[43]
	4.28	[44]
	3.74	[45]
	3.9	[46]
Nb	4.19±0.04	[42]
	4.3	[44]
	3.99	[45]
	4.1	[46]
Nb_2Al (100)	4.02	Calculated

The work function Φ is a parameter for surface, which means the minimum energy required to move an electron from the interior of solid to the surface and can be expressed as follows:

$$\Phi=E_{vac}-E_f \quad (6)$$

where E_{vac} is the vacuum level and E_f is the Fermi level.

The work function of Nb_2Al (100) surface is rarely calculated in other reports and the experimental and theoretical work function of Nb_2Al (100) surface[42-46] of Al and Nb are shown in Table 2. It indicates that the work function of Nb_2Al (100) is close to the work function of pure elements. The work function reflects the difficulty of gaining and losing electrons on the surface of the material. A high work function indicates that it is difficult to lose electrons, suggesting that the surface is more stable and the corrosion resistance is better. Hence, after the Nb_2Al alloy forms, its corrosion resistance is basically unchanged.

3 Conclusions

1) The Nb_2Al (100) surfaces with $Nb_{20}Al_{11}$, $Nb_{21}Al_{12}$, $Nb_{22}Al_{12}$, $Nb_{23}Al_{12}$ and $Nb_{25}Al_{12}$ terminations were analyzed. The shapes of total density of states of all terminated surfaces shift to the right according to the calculated surface electronic structures. The increase of metallic property and the decrease

of covalence appear after the terminated surfaces form.

2) The non-stoichiometric surface energies depend on the chemical potential of Nb. The $Nb_{22}Al_{12}$ termination is the most thermodynamically stable surface under both Nb-rich and Al-rich conditions.

3) According to the calculated work function, the corrosion resistance of the Nb_2Al alloy is similar to that of Al and Nb.

References

1 Glowacki B A. *Intermetallics*[J], 1999, 7(2): 117

2 Luo M, Chen H M, Wang H C *et al*. *The Chinese Journal of Nonferrous Metals*, 2011, 21(1): 73 (in Chinese)

3 Glowacki B A, Yan X Y, Fray D *et al*. *Physica C, Superconductivity*[J], 2002, 372: 1315

4 Miao W, Tao K, Liu B X *et al*. *Nuclear Instruments and Methods in Physics Research Section B: Beam Interactions with Materials and Atoms*[J], 2000, 160(3): 343

5 Kuroda T, Wada H, Iijima Y *et al*. *Journal of Applied Physics*[J], 1989, 65(11): 4445

6 Gauthier V, Josse C, Larpin J P *et al*. *Oxidation of Metals*[J], 2000, 54(1-2): 27

7 Bhattacharya A K. *Journal of the American Ceramic Society*[J], 1992, 75(6): 1678

8 Hanada S. *Current Opinion in Solid State and Materials Science* [J], 1997, 2(3): 279

9 McKinsey C R, Faulring G M. *Acta Crystallographica*[J], 1959, 12(9): 701

10 Leyarovski E, Leyarovska L, Krasnopyorov E *et al*. *Zeitschrift für Physik B Condensed Matter*[J], 1977, 27(1): 57

11 Brown P W, Worzala F J. *Journal of Materials Science*[J], 1976, 11(4): 760

12 Papadimitriou I, Utton C, Tsakiropoulos P *et al*. *Computational Materials Science*[J], 2015, 107: 116

13 Rios C T, Ferrandini P L, Milenkovic S *et al*. *Materials Characterization*[J], 2005, 54(3): 187

14 Rios C T, Ferrandini P, Caram R *et al*. *Materials Letters*[J], 2003, 57(24-25): 3949

15 Liu C T, Stiegler J O. *Science*[J], 1984, 226: 636

16 Rios C T, Milenkovic S, Caram R *et al*. *Journal of Crystal Growth*[J], 2000, 211(1-4): 466

17 Ye F, Mercer C, Soboyejo W O *et al*. *Metallurgical and Materials Transactions A*[J], 1998, 29(9): 2361

18 Jiao H, Barradas F, Rong T *et al*. *Materials Science and Engineering A*[J], 2004, 387: 476

19 Jiao Z, Liu Q J, Liu F S *et al*. *Brazilian Journal of Physics*[J], 2016, 46(2): 213

20 Parameswaran V R. *JOM*[J], 1992, 44(6): 349

21 Clark S J, Segall M D, Pickard C J *et al*. *Zeitschrift für Kristallographie Crystalline Materials*[J], 2005, 220(5-6): 567

22 Vanderbilt D. *Physical Review B*[J], 1990, 41(11): 7892

23 Perdew J P, Chevary J A, Vosko S H *et al*. *Physical Review B*[J], 1992, 46: 6671

24 *Monkhorst H J, Pack J D. Physical Review B*[J], 1976, 13: 5188

25 Liu Q J, Liu Z T. *Vacuum*[J], 2014, 107: 90

26 Liu W, Zheng W T, Jiang Q *et al*. *Physical Review B*[J], 2007, 75(23): 235 322

27 Brown P J, Forsyth J B. *Acta Crystallographica*[J], 1961, 14(4): 362

28 Timusk T, Statt B T. *Reports on Progress in Physics*[J], 1999, 62(1): 61

29 Segall M D, Shah R, Pickard C J *et al*. *Physical Review B*[J], 1996, 54(23): 16 317

30 Wang Y X, Arai M, Sasaki T *et al*. *Physical Review B*[J], 2006, 73(3): 35 411

31 Reuter K, Scheffler M. *Physical Review B*[J], 2001, 65(3): 35 406

32 Zhang W, Smith J R. *Physical Review B*[J], 2000, 61(24): 16 883

33 Chen G H, Hou Z F, Gong X G *et al*. *Computational Materials Science*[J], 2008, 44(1): 46

34 Altarawneh M, Marashdeh A, Dlugogorski B Z *et al*. *Physical Chemistry Chemical Physics*[J], 2015, 17(14): 9341

35 Widjaja H, Miran H A, Altarawneh M *et al*. *Materials Chemistry and Physics*[J], 2017, 201: 241

36 Guerrero-Sánchez J, Mandru A, Wang K *et al*. *Applied Surface Science*[J], 2015, 355: 623

37 Guerrero-Sánchez J, Takeuchi N. *Applied Surface Science*[J], 2016, 390: 328

38 Guerrero-Sánchez J, Mandru A, Takeuchi N *et al*. *Applied Surface Science*[J], 2016, 363: 651

39 Sun S P, Li X P, Wang H J *et al*. *Applied Surface Science*[J], 2014, 288: 609

40 Shilo I, Franzen H F, Schiffman R A *et al*. *Journal of the Electrochemical Society*[J], 1982, 129(7): 1608

41 Gelashvili G A, Dzneladze Z I. *Powder Metallurgy and Metal Ceramics*[J], 1995, 14: 732

42 Wilson R G. *Journal of Applied Physics*[J], 1966, 37(8): 3170

43 Lang N D, Kohn W. *Physical Review B*[J], 1971, 3(4): 1215

44 Michaelson H B. *Journal of Applied Physics*[J], 1977, 48(11): 4729

45 Mohamedi M, Kawaguchi N, Sato Y *et al*. *Journal of Alloys and Compounds*[J], 1999, 287(1-2): 91

46 Hauri C P, Ganter R, Le Pimpec F *et al*. *Physical Review Letters* [J], 2010, 104(23): 234 802

Nb_2Al (100)表面的电子结构和相对稳定性

洪　丹[1,3]，焦　振[1,3]，曾　薇[2]，刘福生[1,3]，唐　斌[4]，刘其军[1,3]

(1. 西南交通大学 物理科学与技术学院 材料先进技术教育部重点实验室，四川 成都 610031)

(2. 成都中医药大学 医学技术学院，四川 成都 610075)

(3. 西南交通大学 高压科学技术四川省高校重点实验室，四川 成都 610031)

(4. 西北工业大学 凝固技术国家重点实验室，陕西 西安 710072)

摘　要：采用基于密度泛函理论的第一性原理计算，研究了Nb_2Al (100)表面不同终止端的电子结构、表面能和热力学性质。计算结果表明，由于表面弛豫和表面态的形成，所有终止端表面的电子结构均表现出增强的金属性质和减弱的共价性质。根据不同终止端表面的表面能计算，分析了非化学计量比表面的稳定性。在富含Nb和Al的条件下，C终止端表面($Nb_{22}Al_{12}$)是热力学最稳定的表面。此外，计算了Nb_2Al (100)表面的功函数，表明该表面获得和失去电子的能力与形成前的纯元素表面相似。

关键词：金属间化合物；密度泛函理论；电子结构；表面性质

作者简介：洪　丹，女，1993年生，博士生，西南交通大学物理科学与技术学院，四川 成都 610031，E-mail：18382927860@163.com